VOL. 20, NO. 18, SEPTEMBER 2025 ISSN 1819-6608
ARPN Journal of Engineering and Applied Sciences

www.arpnjournals.com

METAMATERIAL-BASED TRANSMIT ANTENNA COUPLED TO A COMPACT RECEIVER FOR EFFICIENT WIRELESS POWER TRANSFER TO BIOMEDICAL IMPLANTS

Amine Harhouz[1], Djelloul Aissaoui[1], Abdelhalim Chaabane[2] and Tayeb A. Denidni[3]
[1]Telecommunications and Smart Systems Laboratory, Faculty of Science and Technology, Ziane Achour University of Djelfa Djelfa, Algeria
[2]Laboratoire des Télécommunications-LT, Institut des Télécommunications, Université 8 Mai 1945 Guelma, Guelma, Algeria
[3]Centre-Energie Matériaux et Télécommunications, Institut National de la Recherche Scientifique (INRS), Montreal, Quebec, Canada
E-Mail: amine.harhouz@univ-djelfa.dz

ABSTRACT

This paper presents a new antenna in body system (AIBS) for wireless power transfer applications at the ISM band. The proposed antenna uses planar microstrip technology, providing a compact size, low signal absorbing ratio (SAR), and wide bandwidth, which are the big challenges of AIBS at the ISM band. This design uses a cavity slot antenna based on microstrip technology that resonates at the ISM band 2.45 GHz for an antenna in a body system. The proposed antenna system conforms to an implantable transmit antenna (TX) and a received antenna (RX) with a gap of 30mm. The transmit antenna is designed using a square metamaterial technique to increase the band width and resonant frequency at a certain frequency. Received antenna has been designed based on a cavity gridded slot to achieve a compact size. The transmit antenna uses Rogers RT5880 substrate with a thickness of 1.575mm, while the receive antenna is implemented on Rogers RO3010 substrate with a thickness of 0.25mm. Both structures are optimized for low specific absorption rate (SAR) to enhance the power transfer efficiency (PTE). The proposed design antenna system integrated with human-body tissue, including skin, fat, and muscle, is simulated by using Computer Simulation Technology (CST) software to create a similar environment to the human body. The proposed design was fabricated and measured at 2.45 GHz. The obtained results show good performance in terms of bandwidth of transmit and received antennas (0.9 GHz- 0.200 GHz), gain 4.5 dB, 2.5 dB, and efficiency 88 %, 81%, respectively. The received antenna has a compact size of 6.83mm × 6.5mm. The transmit and receive antennas provide a good VSWR of 1.2 and 1.17, respectively. In addition, the front-to-back radiation ratios of the transmit and receive antennas are 20.4dB and 16.07dB, respectively. Designs have been fabricated and measured with minced pork because it has similar tissue to the human body. Measurement results are in good agreement with simulation results, which validate the proposed antenna designs.

Keywords: antennas in body transmit antennas, received antennas, metamaterials, wireless power transfer.

Manuscript Received 4 August 2025; Revised 15 December 2025; Published 30 December 2025

1. INTRODUCTION

Currently, wireless power transfer (WPT) is widely used in implantable medical devices, eliminating the limitations associated with wired devices [1, 2]. These implantable devices include capsule endoscopes [3], pacemakers for cardiac therapy, and intracranial pressure monitors, which are increasingly utilized for various medical conditions [4]. Medical technologies have been developed to improve the transmission of videos or images [5, 6] by using efficient antennas with good parameters, such as bandwidth, gain, directivity, efficiency, and SAR of transmit and receive antennas. In addition, the development has been focused on the shape and size of the antenna to be suitable for WPT applications with good performance. Several shapes of antennas have been proposed using microstrip technology. The common shapes are rectangular, triangular, square, and circular. These shapes of antenna have been selected to accommodate various applications [7]. Before implanting antennas, there are some requirements that should be considered. First, the life cycle of the antenna that will be implanted in the human body should be as long as possible. Second, the bandwidth of the antenna should be large enough to cover the operating transmit frequency range [8]. Third, the operation frequency should be fixed to cover the desired application. Operating at higher frequency bands will produce heating, which creates a big challenge for medical applications. On the other hand, sometimes we need to go to higher frequencies because all required parameters of the antenna for medical applications are high, such as bandwidth and gain, which means the rate of transmission signal will be high if the parameters of the antenna are high [9]. For instance, in [10], a proposed antenna has achieved multi-band coverage, leading to covering several frequencies. However, this design has achieved a narrow bandwidth at the selected frequency bands. A T-shaped slot has been inserted at the top of the radiation patch antenna that is implanted in the human body. This T-shape makes the antenna radiate at 2.45GHz and 915 MHz [11]. In addition, it is difficult to increase the bandwidth of the proposed design in this paper because of the complex design and its position inside the human body, which cannot change its size or modify its shape. Some researchers have achieved a wider bandwidth at a certain frequency [12]. However, it has a large size and narrow bandwidth, which is challenging for biomedical applications. Several techniques can be used to decrease the size of an antenna; one of them uses a substrate with a higher permittivity constant value to decrease the size of the antenna, as reported in [13]. Another one uses a spiral transmission line as described in [14]. In addition, a slot has been used in [16]. Finally, pins and stacking antennas have been proposed in [17]. However, these methods for decreasing the size of the antenna can also generate some issues related to transmission loss or mismatching, as described in [18]. A capsule shape has been suggested to achieve a compact size for implanting the antenna inside the human body. Some researchers have designed a flexible antenna to give more flexibility for implantation inside the human body; however, these designs have failed to achieve a wider bandwidth at certain frequencies [19]. In [20], a dual-band antenna has been proposed at 2.3 GHz with very low bandwidth, almost 200MHz, and the second bandwidth started from 5.725-5.850 GHz. Another antenna has been designed using microstrip and SIW technology for the biomedical field to transmit and receive signals to achieve a more compact size [21].

This paper presents a new design of a transmit and receive antenna system based on microstrip technology. The transmit antenna incorporates a metamaterial (MTM) structure to enhance the bandwidth and gain, while the receive antenna is designed using a cavity grid slot configuration to achieve a compact size. Both antennas are optimized for high gain and low specific absorption rate (SAR) to enable efficient power transfer over longer distances without affecting the three layers of the body, which are fat, muscle, and skin.

2. DESIGN TRANSMIT AND RECEIVE ANTENNA PROCESS

This section presents the design process and methodology of the proposed transmit and receive antennas using microstrip and metamaterial structures.

The transmit antenna is designed using a square patch fed by a microstrip straight feedline and a cavity slot etched at the top of the patch to increase the radiation area. To improve the proposed antenna design in terms of bandwidth and gain, metamaterials (MTMs) are used in its structure as illustrated in Figure-2. Figure-2 (a) refers to the transmit antenna with MTMs to increase the gain and bandwidth of the antenna.

The MTMs are artificial, effectively homogeneous electromagnetic structures that exhibit novel electromagnetic properties that are not typically found in nature [22]. A structure whose structural average cell size p is much smaller than the quarter wavelength ($p < \lambda g/4$) is known as an effectively homogeneous structure. MTMs are a type of artificially constructed material dependent on periodical structures, materials with negative permittivity and permeability at the same time, thereby they are known as Double Negative Metamaterial (DNM), as shown in Figure-1. In Figure-1, isotropic dielectrics, plasmas, and ferromagnetic compounds are the materials that exist in quadrants I, II, and IV, respectively. All of them are well known in conventional materials, though negative permittivity and permeability of materials in quadrants III have not yet been observed in nature. Figure-1 shows the classification of materials based on the values of permittivity ε and permeability μ. The quadrant I ($\varepsilon > 0$, $\mu > 0$) represents the right-handed material (RHM). In the first quadrant, the forward propagation of the wave takes place, and the group and phase velocities are in the same direction. The material is widely used and follows the rule of the right-handed (RH) thumb for the direction of wave propagation. Electric plasmas supporting evanescent waves are described in quadrant II ($\varepsilon < 0$ and $\mu > 0$) and are also called epsilon negative (ENG) materials. Quadrant IV, which represents $\varepsilon > 0$ and $\mu < 0$, describes ferromagnetic material supporting evanescent waves, and it is also called as mue μ-negative (MNG) material [23].

Figure-2 (b) shows the receive antenna. A microstrip square patch with thickness 0.25mm, permittivity 2.2, and loss 0.0009 is designed using the Roger RO3010 substrate. The proposed design has a full ground plane covered, and the power of the receive antenna is fed from the bottom. For a smaller antenna, a cavity slot is inserted in the top layer of the patch to increase the gain and reduce the antenna size. All of the transmit and receive antenna dimensions are listed in Table-1.

ARPN Journal of Engineering and Applied Sciences

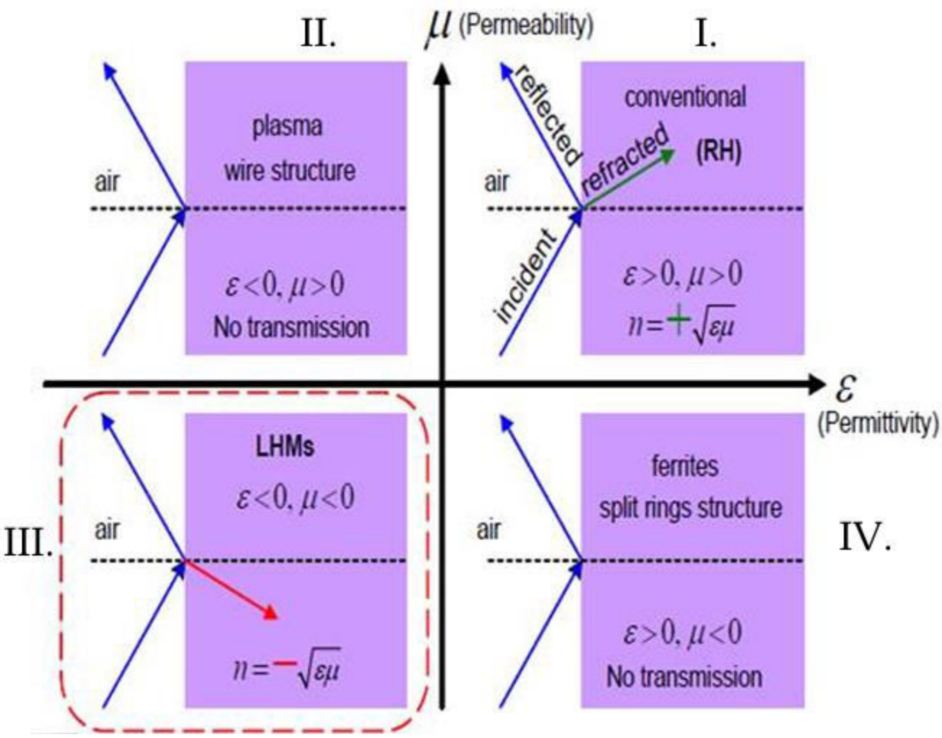

Figure-1. Classification of materials based on the value of permittivity ε and permeability μ [23].

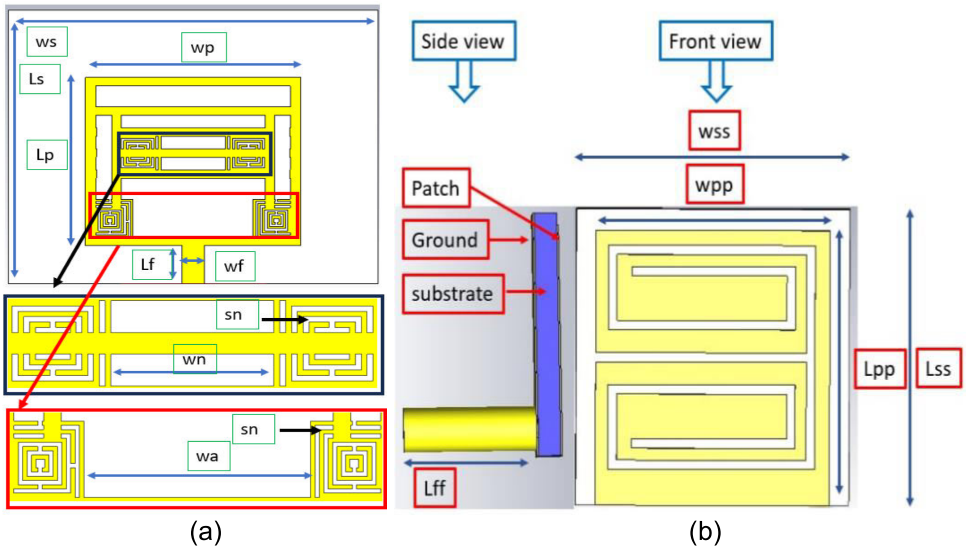

Figure-2. Geometry of the proposed antennas with metamaterials, (a) Transmit antenna, (b) Receive antenna.

ARPN Journal of Engineering and Applied Sciences

Table-1. The dimensions of the transmit and receive antennas.

Transmit antenna			Receive antenna		
Simple	**Explanation**	**Value (mm)**	**Simple**	**Explanation**	**Value (mm)**
Ws	Width of substrate	80	wss	Width of substrate	6.5
Ls	Length of substrate	65	wpp	Width of patch	6
wp	Width of patch	40	Lss	Length of substrate	6.83
Lp	Length of patch	46	Lpp	Length of patch	6.5
Wf	Width of feedline	1.57	Lff	Length of feeder	3
Lf	Length of feedline	9			
Sn	Size of MTM slot	0.5	Patch	Thickness of the patch	0.035
Wn	Distance between two cells	14	Ground	Thickness of the ground	0.035
wa	Distance between two cells	26	substrate	Thickness of substrates	0.25

3. INTEGRATION OF TRANSMIT AND RECEIVE ANTENNAS

After designing the transmit and receive antennas at 2.45 GHz, this section aims to integrate both the transmit and receive antennas within the body system, involving miniaturized, biocompatible antennas that can be safely implanted. These antennas must be strategically placed to ensure optimal signal transmission and reception while minimizing interference with bodily functions. The choice of the frequency bands is crucial, as lower frequencies penetrate tissues better but require larger antennas, whereas higher frequencies offer better data rates but face higher attenuation. Power management is another key aspect, often involving energy harvesting techniques or external power sources to avoid large batteries. Advanced signal processing is essential to filter out noise and ensure secure data transmission. Thorough testing, both in simulated environments and in vivo, is necessary to validate the system's performance and compliance with medical standards. Figure-3 refers to the integration of transmit and receive antennas, where the receive antenna is placed inside three layers of the human body, which are skin, fat, and muscle.

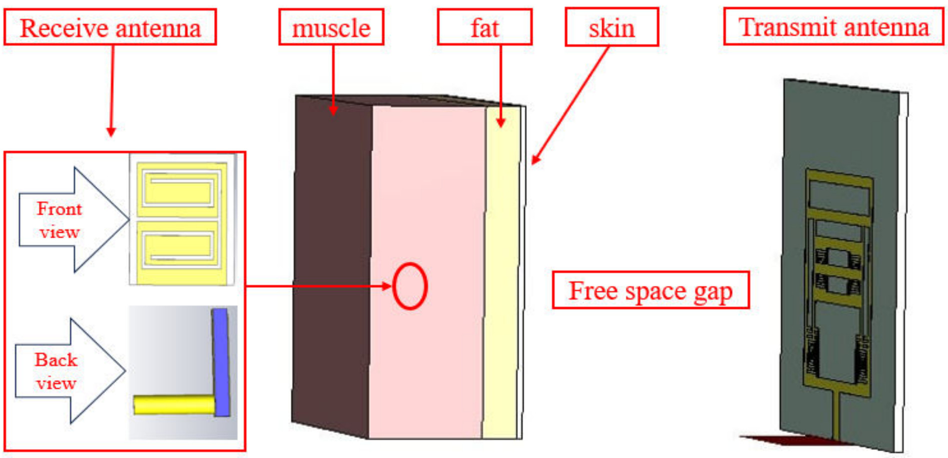

Figure-3. Integration of transmit and receive antennas in the body.

4. FABRICATION PROCESS OF TX AND RX

The prototype of the design was fabricated and measured once the proposed designs had been finalized. All of the designs were fabricated using a Roger RT board with a thickness of 1.575 mm and a dielectric constant (εr) of 2.2. JAC Engineering, Malaysia, conducted the fabrication process. The wet etching PCB fabrication technique was performed for the fabrication of all the components used in this research study. The most challenging aspect is the soldering of the SMA conductor, as good soldering skills are needed in order to obtain good measurement results. Multiple times, SMA soldering has been performed on the feed line of different fabricated

ARPN Journal of Engineering and Applied Sciences

prototypes. Figure (a) refers to the transmit antenna, and Figure (b) refers to the receive antenna.

The measurement of the components was made after the fabrication process was completed. All of these measurements were carried out using Keysight (Agilent Technologies) FieldFox N9925A vector network analyzer (VNA). The performance parameters such as reflection coefficient, gain, and radiation pattern.

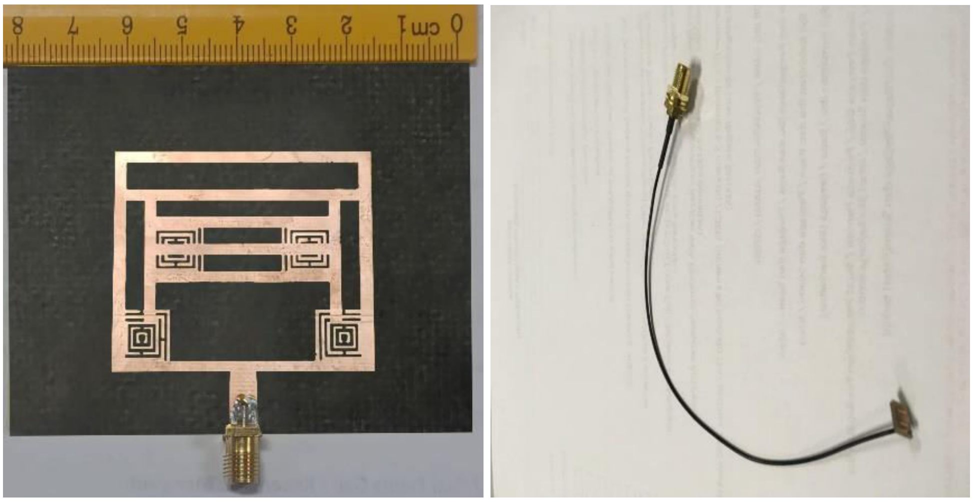

(a) (b)

Figure-4. Fabricated design of WPT, (a) transmit antenna, (b) receive antenna.

5. RESULTS AND DISCUSSIONS

The reflection coefficient, often denoted as the transmit propagation, is a critical parameter in antenna design. It measures the fraction of the incident electromagnetic wave that is reflected due to impedance mismatch at the antenna's input. The reflection coefficient values indicate how well the antenna is matched to the transmission line. A lower reflection coefficient signifies better matching and, consequently, higher efficiency. The reflection coefficient of the transmit antenna (TX) achieves a large bandwidth of 1GHz at the operating frequency of 2.45GHz. As mentioned in the previous section, MTM unit cells are used in the TX to increase the bandwidth, providing a resonant frequency (S11 of -16 dB) at 2.45 GHz, as shown in Figure-5. The receive antenna (RX) achieves good matching at 2.45 GHz (s11=-28 dB as illustrated in Figure-5). Furthermore, the RX antenna design has a compact size thanks to using a cavity grid slot configuration in the top layer of the antenna, which can be placed inside the human body. The transmit antenna is placed in free space, and the receive antenna is inserted in the body to achieve integration of wireless propagation in the body between the TX and RX antennas. As can be seen in Figure-6, this wireless integration achieves good matching, the reflection coefficient of integration achieves a wide band of 0.9 GHz with -18 dB around the frequency of 2.45 GHz. S21 of integration TX and RX achieves a wide frequency band from 2 to 2.8 GHz, covering the ISM BAND easily around 2.45 GHz, as shown in Figure-5 (a). After fabricating the proposed design of TX and RX antennas, the transmit and receive antennas were measured using a vector network analyzer (VNA). The reflection coefficients of TX and RX antennas are -15 dB and -24 dB, respectively. The reflection coefficient of integration TX and RX antennas is -15 dB at 2.45 GHz. Furthermore, S21 achieves -11 dB at the range frequency from (2.2-2.8) GHz, as shown in Figure-5 (b). A slight difference between experimental results and simulated ones is due to the losses of cables, tolerance of fabrication, and measurement errors.

The gain of a transmitting antenna describes its ability to convert the input power into radio waves directed towards a specific direction. This parameter is crucial because it determines how effectively the antenna can radiate power in the desired direction. A high-gain antenna focuses the radiated power into a narrow beam, which increases the signal strength in that direction. This is beneficial for long-distance communication as it enhances the effective range. Figure-6 (a) refers to the TX and RX gain as simulated and measured results; the transmit antenna achieves a measured gain of 3.3 dB and a simulated one of 3dB at 2.45 GHz. The receive antenna achieves simulated and measured gains of 2.5 dB and 2.3 dB at 2.45 GHz, respectively. The antenna efficiency is a crucial parameter that indicates how effectively an antenna converts the input power into radiated electromagnetic waves. It is defined as the ratio of the power radiated by the antenna to the total input power supplied to it. Figure-6 (b) refers to the TX and RX simulated and measured efficiency; the transmit antenna achieves simulated and measured efficiency 88% and 84 % at 2.45 GHz, respectively. The receive antenna achieves simulated and measured efficiency of 82 % and 80% at 2.45 GHz, respectively.

VOL. 20, NO. 18, SEPTEMBER 2025 ISSN 1819-6608
ARPN Journal of Engineering and Applied Sciences

www.arpnjournals.com

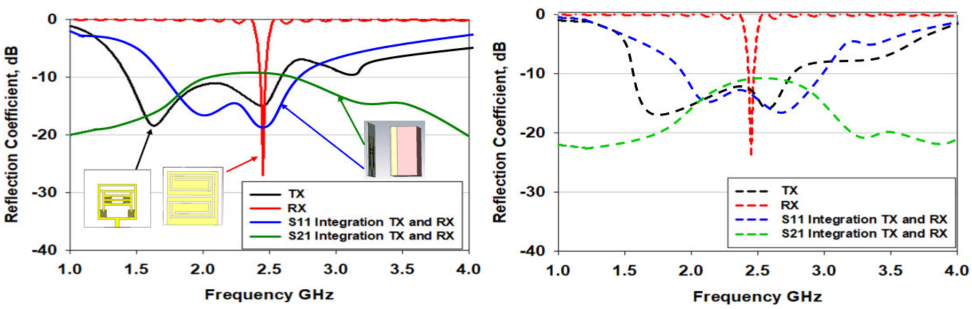

(a) (b)

Figure-5. Reflection coefficient of the proposed three designs,
(a) simulated results, (b) measured results.

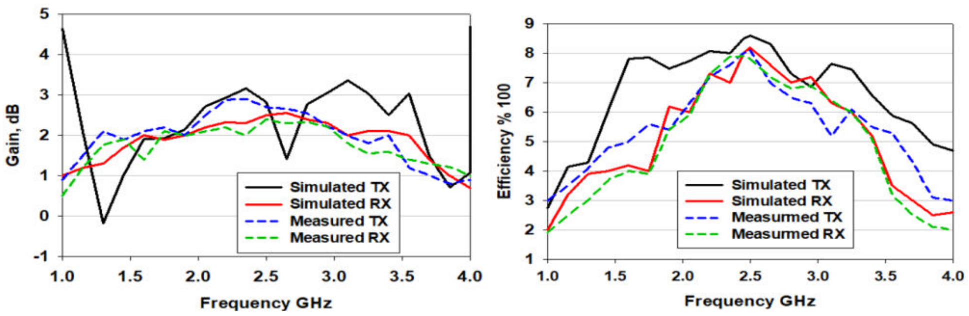

(a) (b)

Figure-6. Measurement of the proposed transmit and receive antenna,
(a) gain, (b) efficiency.

The polar radiation pattern of an antenna is a graphical representation that shows how the antenna radiates power in different directions. This pattern is crucial for understanding the performance and behavior of the antenna in its intended application. Figure-7 refers to the simulated and measured radiation patterns in the E- and H-planes of TX and RX antennas. Figure-7 (a) shows the simulated and measured radiation pattern in the E-plane of the proposed TX and RX antennas, with a low side lobe and directive beam. Furthermore, Figure-7 (b) shows the simulated and measured radiation pattern in the H-plane of the proposed TX and RX antennas, indicating an omnidirectional beam. Figure-8 illustrates the 3D radiation pattern of the proposed TX and RX antennas. Table-2 provides the comparison results between the proposed work and related previous contributions in the literature.

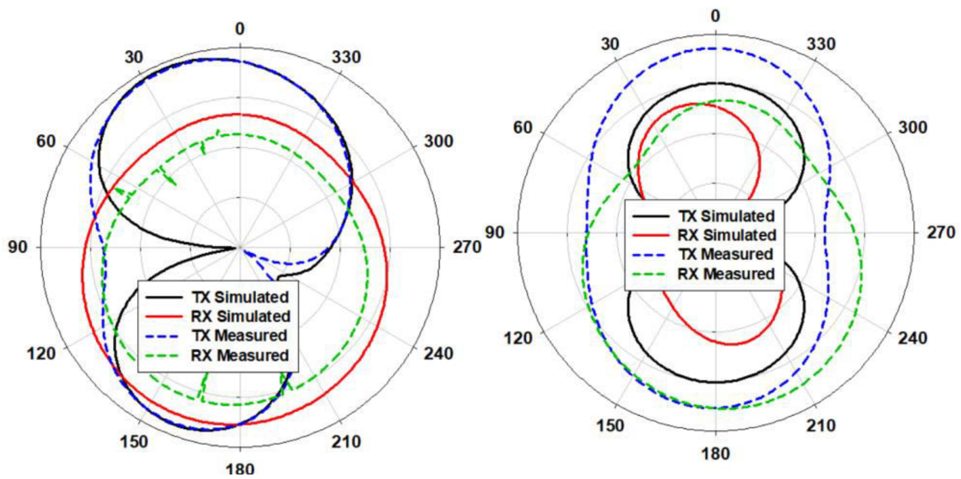

(a) (b)

Figure-7. Radiation pattern of the proposed TX and RX antennas,
(a) E palne, (b) H plane.

VOL. 20, NO. 18, SEPTEMBER 2025 ISSN 1819-6608
ARPN Journal of Engineering and Applied Sciences

www.arpnjournals.com

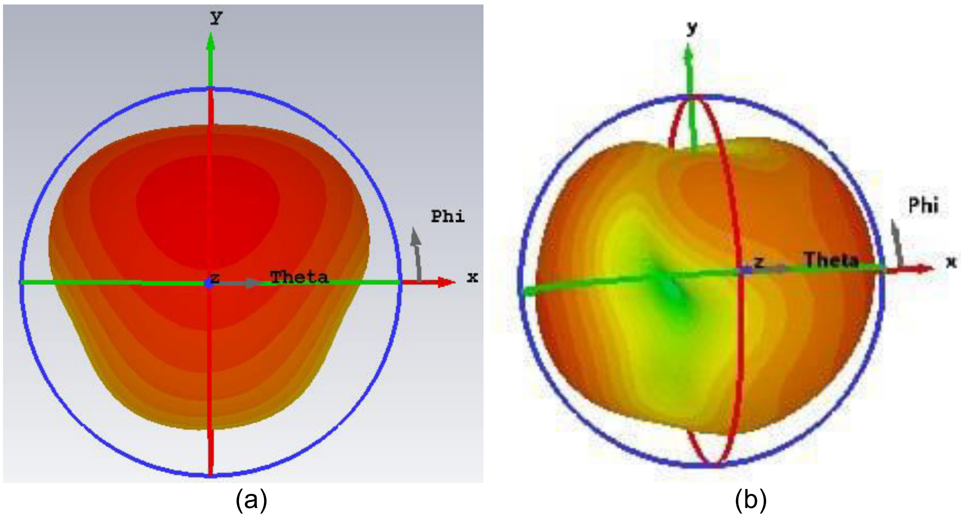

Figure-8. 3D radiation pattern of TX and RX antennas, (a) transmit antenna (TX), (b) receive antenna (RX).

Table-2. Comparison results of the antenna in the body with the antenna in this paper.

Ref	Year	Freq	Dimension (mm^3)	Substrate	εr	Thickness (mm)	Depth (mm)	Gain (dBi)	SAR (W/kg)	Antenna type
[24]	2014	2.4GHz	10 × 10 × 1.27	Rogers 3010	10.2	0.635	4 skins	-22	213	Conformal
[25]	2014	2.4GHz	10 × 5.5 × 3.81	Rogers 3010	10.2	0.635	50 muscle	-32	599	Conformal
[26]	2016	2.4GHz	10 × 10 × 1.27	Rogers 3010	10.2	0.635	5 muscles	-22.33	350	Conformal
[27]	2017	2.4GHz	8.5 × 8.5 × 1.27	Rogers 3010	10.2	0.635	4 skins	-27	200	Embedded
[28]	2017	915 MHz	15 × 15 × 1.27	Rogers 3010	10.2	0.635	3 skins	-32	517	Embedded
[29]	2018	915 MHz	11 × 11 × 1.27	Rogers 3010	10.2	0.635	4 skins	-29	N\A	Conformal
[30]	2019	402–405 MHz	7 × 6.5 × 0.377	Rogers 6010	9.8	0.2	3 skins	-30.22	66	Embedded
[31]	2020	402 915 1200	10 × 10 × 1.27	ULTRALAM	2.9	0.1	5 muscles	-30.8 -19.7 -18.7	60.9 53.9 50.5	Conformal
[32]	2020	2.4GHz	22 × 23 × 1.27	Rogers 6010	10.2	1.2	3 skins	-36	64	Embedded
[33]	2021	2.4GHz	25 × 25 × 1.28	Rogers 3210	10.2	0.25	3 skins	-18.33	36	Conformal
[21]	2022	2.4 GHz 5.8 GHz	11 × 25 × 1.28	Rogers 5880	2.20	0.787	5 muscle	-7.5 -5.1	39.9 14.7	Conformal
This work	2025	2.45	6.83×6.5×0.32	Rogers 3010	2.2	0.25	3 skins	3.4	12.3	Conformal

As shown in Table-1, implantable and conformal antenna designs intended for wireless power transfer (WPT) in biomedical applications have undergone significant development over the past decade. In early works between 2014 and 2016, antennas with dimensions around 10 × 10 mm were commonly used, employing high-permittivity substrates such as Rogers 3010 (εr = 10.2) [24-26]. However, these designs suffered from highly negative gain values (ranging from -22 to -36 dBi) and extremely high specific absorption rate (SAR) levels, reaching up to 599 W/kg, making them inefficient in terms of power transfer and biologically unsafe. With gradual research progress between 2017 and 2020, notable improvements began to emerge [27-32]. These included the use of lower frequencies such as 402 MHz to enhance penetration depth into tissues, as well as the adoption of low-permittivity materials to extend the operational bandwidth and reduce SAR levels. In recent years, modern designs have focused on reducing SAR while achieving noticeable improvements in gain, alongside the continued use of low-permittivity substrates to enhance efficiency and minimize energy losses [21, 33]. In comparison with these previous works, the proposed work also features a reduction in the overall size of the receiver antenna, further improving its suitability for implantation within biological tissues.

6. CONCLUSIONS

In this paper, the design, implementation, and performance of implantable antennas for biomedical applications have been explored. The obtained results have demonstrated that implantable antennas can effectively facilitate wireless communication within the human body, overcoming significant challenges such as miniaturization, biocompatibility, and efficient signal transmission through various tissues. The proposed antenna designs have shown promising results in terms of radiation efficiency, bandwidth, and patient safety with low SAR. By optimizing the antenna's size and material, we have achieved a balance between performance and biocompatibility, ensuring minimal tissue damage and reliable data transmission. The transmit antenna (TX) and receive antenna (RX) have been simulated, fabricated, and measured. The obtained results have shown good performance at 2.45 GHz for WPT applications.

REFERENCES

[1] R. Shadid and S. Noghanian. 2018. A Literature Survey on Wireless Power Transfer for Biomedical Devices. Int. J. Antennas Propag., vol. 2018, doi: 10.1155/2018/4382841.

[2] M. M. Soliman *et al*. 2021. Review of medical implantable antenna technology and imminent research challenges. Sensors, 21(9), doi: 10.3390/s21093163.

[3] R. Alrawashdeh. 2020. Patch antenna based on spiral split rings for bone implants. Prz. Elektrotechniczny, 96(7): 129134, doi: 10.15199/48.2020.07.24.

[4] N. Dixit, A. Agarwal, and K. Patkar. 2016. Implementation of multiple square slots in a micro-strip rectangular patch antenna for S-band application. In 2016 Symposium on Colossal Data Analysis and Networking (CDAN), pp. 1-3, doi: 10.1109/CDAN.2016.7570931.

[5] Z. Bao, Y. X. Guo, and R. Mittra. 2018. Conformal Capsule Antenna with Reconfigurable Radiation Pattern for Robust Communications. IEEE Trans. Antennas Propag., 66(7): 3354-3365, doi: 10.1109/TAP.2018.2829828.

[6] P. Loktongbam, D. Pal, and C. Koley. 2020. Design of an implantable antenna for biotelemetry applications. Microsyst. Technol., 26(7): 2217-2226, doi: 10.1007/s00542 019-04531-y.

[7] M. M. Jawad, N. N. N. A. Malik, N. A. Murad, M. R. Ahmad, M. R. M. Esa, and Y. M. Hussein. 2020. Design of substrate integrated waveguide with Minkowski-Sierpinski fractal antenna for wban applications. Bull. Electr. Eng. Informatics, 9(6): 2455-2461, 2020, doi: 10.11591/eei.v9i6.2194.

[8] S. Ahmad *et al*. 2022. A Wideband Bear-Shaped Compact Size Implantable Antenna for In-Body Communications. Appl. Sci., 12(6): doi: 10.3390/app12062859.

[9] Mansoor, Riyadh, *et al*. 2015. Crosstalk bandwidth of grating-assisted ring resonator add/drop filter. Optical and quantum electronics. 47: 1127-1137.

[10] Mansoor, Riyadh, *et al*. 2015. Crosstalk suppression bandwidth optimisation of a vertically coupled ring resonator add/drop filter. IET optoelectronics. 92: 30-36.

[11] A. J. A. Al-Gburi *et al*. 2021. High Gain of UWB CPW-fed Mercedes-shaped printed monopole antennas for UWB applications. Prz. Elektrotechniczny, 97(5): 70-73, doi: 10.15199/48.2021.05.11.

[12] M. S. Miah, A. N. Khan, C. Icheln, K. Haneda, and K. Takizawa. 2018. Antenna Systems for Wireless Capsule Endoscope: Design, Analysis, and Experimental Validation. pp. 1-11, [Online]. Available: http://arxiv.org/abs/1804.01577.

[13] S. Hout and J. Y. Chung. 2019. Design and Characterization of a Miniaturized Implantable Antenna in a Seven-Layer Brain Phantom. IEEE Access, 7(November): 162062-162069, doi: 10.1109/ACCESS.2019.2951489.

[14] N. Ganeshwaran, J. K. Jeyaprakash, M. G. N. Alsath, and V. Sathyanarayanan. 2020. Design of a Dual-Band Circular Implantable Antenna for Biomedical Applications. IEEE Antennas Wirel. Propag. Lett., 19(1): 119-123, doi: 10.1109/LAWP.2019.2955140.

[15] F. Faisal, M. Zada, A. Ejaz, Y. Amin, S. Ullah, and H. Yoo. 2020. A Miniaturized Dual-Band Implantable Antenna System for Medical Applications. IEEE Trans. Antennas Propag., 68(2): 1161-1165, doi: 10.1109/TAP.2019.2938591.

[16] S. Symeonidis, W. G. Whittow, M. Zecca, and C. Panagamuwa. 2018. Bone fracture monitoring using implanted antennas in the radius, tibia, and phalange

heterogeneous bone phantoms. Biomed. Phys. Eng. Express, 4(4), doi: 10.1088/2057-1976/aab974.

[17] Z. Xia *et al*. 2020. A Wideband Circularly Polarized Implantable Patch Antenna for ISM Band Biomedical Applications. IEEE Trans. Antennas Propag., 68(3): 2399-2404, doi: 10.1109/TAP.2019.2944538.

[18] S. Ahmad, B. Manzoor, S. Naseer, N. Santos-Valdivia, A. Ghaffar, and M. I. Abbasi. 2022. X-Shaped Slotted Patch Biomedical Implantable Antenna for Wireless Communication Networks. Wireless. Commun. Mob. Comput., vol. 2022, doi: 10.1155/2022/7594587.

[19] D. Nikolayev, W. Joseph, A. Skrivervik, M. Zhadobov, L. Martens, and R. Sauleau. 2019. Dielectric-Loaded Conformal Microstrip Antennas for Versatile In-Body Applications. IEEE Antennas Wirel. Propag. Lett., 18(12): 2686-2690, doi: 10.1109/LAWP.2019.2948814.

[20] M. S. Singh, J. Ghosh, S. Ghosh, and A. Sarkhel. 2021. Miniaturized Dual-Antenna System for Implantable Biotelemetry Application. IEEE Antennas Wirel. Propag. Lett., 20(8): 1394-1398, doi: 10.1109/LAWP.2021.3081477.

[21] Jawad, Mustafa Mohammed. 2023. Design of a Conformal Fractal Antenna with SIW for Medical Implants Application. Przegląd Elektrotechniczny: n. Pag.

[22] Xu H., Wang G., Liang J., *et al*. 2013. Compact Circularly Polarized Antennas Combining Meta-Surfaces and Strong Space-Filling Meta-Resonators. IEEE Transactions on Antennas and Propagation. 61: 3442-3450.

[23] He S. 2007. Electromagnetic Metamaterials: Transmission Line Theory and Microwave Applications. By Christophe Caloz and Tatsuo Itoh. ChemPhysChem. 8: 618-619.

[24] C. Liu, Y. X. Guo, and S. Xiao. 2014. Capacitively loaded circularly polarized implantable patch antenna for ISM band biomedical applications. IEEE Trans. Antennas Propag., 62(5): 2407-2417, doi: 10.1109/TAP.2014.2307341.

[25] H. Li, Y. X. Guo, and S. Q. Xiao. 2016. Broadband circularly polarised implantable antenna for biomedical applications. Electron. Lett. 52(7): 504-506, doi: 10.1049/el.2015.4445.

[26] X. Y. Liu, Z. T. Wu, Y. Fan and E. M. Tentzeris. 2017. A Miniaturized CSRR-Loaded Wide-Beamwidth Circularly Polarized Implantable Antenna for Subcutaneous Real-Time Glucose Monitoring. IEEE Antennas Wirel. Propag. Lett., 16(c): 577-580, doi: 10.1109/LAWP.2016.2590477.

[27] K. Zhang, C. Liu, X. Liu, H. Guo, and X. Yang. 2017. Miniaturized Circularly Polarized Implantable Antenna for ISM-Band Biomedical Devices. Int. J. Antennas Propag., vol. 2017, doi: 10.1155/2017/9750257.

[28] C. Liu, Y. Zhang, and X. Liu. 2018. Circularly Polarized Implantable Antenna for 915 MHz ISM-Band Far-Field Wireless Power Transmission. IEEE Antennas Wirel. Propag. Lett., 17(3): 373-376, doi: 10.1109/LAWP.2018.2790418.

[29] N. Pournoori, S. Ma, L. Sydanheimo, L. Ukkonen, T. Bjorninen and Y. Rahmat-Samii. 2019. Compact dual-band PIFA based on a slotted radiator for wireless biomedical implants. 2019 IEEE Int. Symp. Antennas Propag. Usn. Radio Sci. Meet. APSURSI 2019 - Proc., (October): 13-14, doi: 10.1109/APUSNCURSINRSM.2019.8889083.

[30] Y. Alamgir *et al*. 2020. Compacted Conformal Implantable Antenna with Multitasking Capabilities for Ingestible Capsule Endoscope. IEEE Access, 8: 157617-157627, doi: 10.1109/ACCESS.2020.3019663.

[31] D. Nguyen and C. Seo. 2021. An ultra-miniaturized antenna using the loading circuit method for medical implant applications. IEEE Access, 9: 111890-111898, doi:10.1109/ACCESS.2021.3103827.

[32] K. Liu *et al*. 2021. Design of Conformal Spiral Dual-Band Antenna for Wireless Capsule System. IEEE Access, vol. pp, 2021, doi: 10.1109/ACCESS.2021.3106735.